Data in Brief 48 (2023) 109101

Contents lists available at ScienceDirect

Data in Brief

journal homepage: www.elsevier.com/locate/dib

Data Article

Data on ADME parameters of bisphenol A and its metabolites for use in physiologically based pharmacokinetic modelling

Barbara Wiśniowska[a], Susanne Linke[b,c], Sebastian Polak[a,d], Zofia Bielecka[a,d], Andreas Luch[b,c], Ralph Pirow[b,*]

[a] Faculty of Pharmacy, Jagiellonian University Medical College, Medyczna 9 Street, 30-688 Kraków, Poland
[b] German Federal Institute for Risk Assessment (BfR), Department of Chemical and Product Safety, Max-Dohrn-Straße 8-10, 10589 Berlin, Germany
[c] Department of Biology, Chemistry, Pharmacy, Institute of Pharmacy, Freie Universität Berlin, Berlin, Germany
[d] Simcyp Division, Certara UK Limited, Level 2-Acero, 1 Concourse Way, Sheffield S1 2BJ, UK

Abbreviations: ADAM, advanced dissolution, absorption and metabolism; ADME, absorption, distribution, metabolism, excretion; AUC, area under the concentration-time curve; B/P ratio, blood-to-plasma concentration ratio; BPA, bisphenol A; BPAG, glucuronidated BPA; BPAS, sulfated BPA; BW, body weight; CES, carboxylesterase; C_{max}, maximum concentration in plasma; CL_{int}, *in vitro* intrinsic clearance; CL_{iv}, total intravenous clearance; CL_{perm}, permeability clearance; CL_{renal}, renal clearance; $CL_{int,bile}$, *in vitro* intrinsic biliary clearance; $CLu_{int,G}$, net intrinsic metabolic clearance in the gut based on unbound BPA concentration; $CL_{int,gutlumen}$, gut lumen intrinsic clearance; EHR, enterohepatic recirculation; f_a, fraction absorbed; fu_{gut}, fraction of BPA unbound in the enterocyte; fu_{inc}, fraction unbound in *in vitro* incubation; fu_{mic}, fraction unbound in microsomal incubation; fu_p, fraction unbound in plasma; F_g, fraction of BPA escaping gut metabolism; HBD, number of hydrogen bond donors; HPGL, hepatocytes per gram of liver; IV, intravenous; IVIVE, *in vitro* to *in vivo* extrapolation; k_a, absorption rate constant; K_a, acid dissociation constant; K_m, Michaelis-Menten constant; K_p, tissue-to-plasma partition coefficient; MechPeff, mechanistic permeability; MPPGL, microsomal protein per gram of liver; MW, molecular weight; Q_{gut}, hybrid parameter of blood flow and compound permeability through enterocytes; QSAR, quantitative structure-activity relationship; *P*, octanol:water partition coefficient; P_{app}, apparent permeability; $P_{eff,man}$, effective intestinal permeability in human; PBPK, physiologically based pharmacokinetics; PSA, polar surface area; RAF, relative activity factor; rhUGT, recombinant human UGT; SULT, sulfotransferase; UGT, UDP-glucuronosyltransferase; V_{max}, maximum velocity; V_{ss}, volume of distribution at steady-state.

DOI of original article: 10.1016/j.taap.2022.116357

* Corresponding author at: Department of Chemical and Product Safety, German Federal Institute for Risk Assessment (BfR), Max-Dohrn-Straße 8-10, 10589 Berlin, Germany.

E-mail addresses: b.wisniowska@uj.edu.pl (B. Wiśniowska), susanne.linke@bfr.bund.de (S. Linke), sebastian.polak@uj.edu.pl (S. Polak), zofia.tylutki@uj.edu.pl (Z. Bielecka), andreas.luch@bfr.bund.de (A. Luch), ralph.pirow@bfr.bund.de (R. Pirow).

https://doi.org/10.1016/j.dib.2023.109101

ARTICLE INFO

Article history:
Received 24 January 2023
Revised 11 March 2023
Accepted 24 March 2023
Available online 30 March 2023

Dataset link: Data for: Data on ADME parameters of bisphenol A and its metabolites for use in physiologically based pharmacokinetic modelling (Original data)

Keywords:
BPA
Bisphenol A
PBPK
ADME
Modelling
Oral route

ABSTRACT

The paper presents the collection of physicochemical parameters of bisphenol A (BPA) and its sulfate (BPAS) and glucuronide (BPAG) conjugates, accompanied by data characterizing their absorption, distribution, metabolism and excretion (ADME) behavior following oral administration of BPA. The data were collected from open literature sources and publicly available databases. Additionally, data calculated by using the MarvinSketch 18.30.0 software or predicted by relevant QSAR models built in Simcyp® Simulator were also used. All data were analysed and are fit for purpose if necessary to ensure a reliable prediction of pharmacokinetics of BPA and its conjugates. The data selection process and reasoning for fitting is provided to allow critical assessment and to ensure data transparency. Finally, the sensitivity analysis was performed to assess the influence of the selected parameters on the PBPK model predictions.

Specifications Table

Subject	Health, Toxicology and Mutagenesis
Specific subject area	Physiologically based pharmacokinetic (PBPK) modelling
Type of data	Table, Figure, Dataset, Simcyp workspace, R script
How the data were acquired	Data were acquired via review of the available literature sources and databases, and predicted using QSAR models.
Data format	Raw, Analysed, Processed
Description of data collection	Data on compounds' physicochemical and ADME properties were collected from published articles, reports, databases (Pubchem) and web documents, calculated in MarvinSketch 18.30.0 (http://www.chemaxon.com), or were predicted by the use of Simcyp built-in QSAR models. Primary (i.e., raw) data involving simulated data on blood concentrations and cumulative urinary excretions were predicted using Simcyp® Simulator V21. Secondary data involving experimental toxicokinetic data for PBPK model verification were obtained from available literature sources.
Data source location	Institution: German Federal Institute for Risk Assessment (BfR) City: Berlin Country: Germany Secondary were obtained from the following primary data sources: K.A. Thayer, D.R. Doerge, D. Hunt, S.H. Schurman, N.C. Twaddle, M.I. Churchwell, S. Garantziotis, G.E. Kissling, M.R. Easterling, J.R. Bucher, L.S. Birnbaum, Pharmacokinetics of bisphenol A in humans following a single oral administration, Environ Int 83 (2015) 107-15. https://doi.org/10.1016/j.envint.2015.06.008 X. Yang, D.R. Doerge, J.G. Teeguarden, J.W. Fisher, Development of a physiologically based pharmacokinetic model for assessment of human exposure to bisphenol A. Toxicol Appl Pharmacol 289 (2015), 442-456. https://doi.org/10.1016/j.taap.2015.10.016 J.G. Teeguarden, N.C. Twaddle, M.I. Churchwell, X. Yang, J.W. Fisher, L.M. Seryak, D.R. Doerge, 24-hour human urine and serum profiles of bisphenol A: Evidence against sublingual absorption following ingestion in soup, Toxicol Appl Pharmacol 288(2) (2015) 131-42. https://doi.org/10.1016/j.taap.2015.01.009

(*continued on next page*)

Data accessibility	The data is available through the Mendeley Data repository at: https://doi.org/10.17632/t7t8kbjpyg.1
Related research article	B. Wiśniowska, S. Linke, S. Polak, Z. Bielecka, A. Luch, R. Pirow, Physiologically based modelling of dermal absorption and kinetics of consumer-relevant chemicals: A case study with exposure to bisphenol A from thermal paper. Toxicol Appl Pharmacol 459 (2023). https://doi.org/10.1016/j.taap.2022.116357

Value of the Data

- The data allow parametrization of intravenous and oral PBPK models for bisphenol A and its conjugates.
- Such models can support human health risk assessment of BPA and can be applied to test different oral exposure scenarios.
- This dataset can also be used to develop PBPK models for other routes of exposure such as the dermal route, as the compound files can be extended for additional parameters.
- The generated data set can be of interest to toxicologists evaluating xenobiotic exposure, regulatory agencies involved in food and chemical risk assessment, and academics interested in the oral and dermal toxicokinetics of xenobiotics.

1. Objective

The data set was generated to develop a physiologically based pharmacokinetic (PBPK) model that supports the human health risk assessment of bisphenol A (BPA), the interpretation of human biomonitoring data, and the establishment of the relationship between external and internal measures of exposure. The iterative modelling process involved the parametrization of BPA and its conjugates (compound models), development of a PBPK model for intravenous administration, and its extension for oral and finally dermal exposure. We considered the data on the physicochemical properties and on absorption, distribution, metabolism and excretion (ADME) parameters of BPA and its sulfate (BPAS) and glucuronide (BPAG) conjugates. Regarding absorption, the focus of this paper is on intravenous and oral models, which were not primarily relevant for the companion paper on PBPK modelling of dermal BPA absorption [1]. However, the generated data can be used to parameterize PBPK models testing various BPA oral exposure scenarios, thus they will be of interest for toxicologists and consumer health protection agencies.

2. Data Description

The collected data set contains information required for the parametrization of the PBPK model for BPA and its conjugates (BPAG and BPAS). The variables considered necessary for model development comprised physicochemical and blood-binding parameters as well as ADME parameters. All data are presented in tables with relevant units and references to the sources or methods of calculation. This set of parameters was used to implement the PBPK model in Simcyp® Simulator V21.

Details on parameterization are given in section Experimental Design, Materials and Methods. Tables 1 and 2 list the parameter estimates for BPA, BPAG, and BPAS. Table 3 provides the parameters for the first-order absorption model, which was one of the two models employed for the oral route of administration. Table 4 provides the trial design parameters of the two clinical studies used for PBPK model refinement and verification. To improve model predictions, we additionally used the advanced dissolution, absorption and metabolism (ADAM) model for the oral route [2]. The switch to the ADAM model required optimization of three ADME parameters and the activation of enterohepatic recirculation (EHR) involving the specification of two additional parameters (Table 5).

Table 1
Physicochemical properties, blood binding and ADME parameters of BPA.

Parameter	Input value	Source / Comment
Physicochemical properties		
MW (g/mol)	228.29	Pubchem
log *P*	3.32	Pubchem (experimental)
pK_a	9.8, 10.4 (diprotic acid)	calculated in MarvinSketch
Blood		
B/P ratio	1.05	predicted in PK-Sim
fu_p	0.0476	experimental value [5], predominantly binding to HSA
Distribution		
Model	Full PBPK model	
Method	Simcyp Method 2	Rodgers and Rowland method
K_p scalar	0.42	manually adjusted
V_{ss} (L/kg)	1.8	allometric scaling [6]
Elimination		
UGT1A9		Recombinant enzyme kinetics [7]
V_{max} (pmol/min/mg)	1000	
K_m (µM)	25	
fu_{mic}	0.25	optimized (initial guess: 0.5)
rhUGT Scalar – Liver	3.22	see text
rhUGT Scalar – Intestine	0.61	= 3.22 × 0.19
rhUGT Scalar – Kidney	8.21	= 3.22 × 2.55
UGT2B15		recombinant enzyme kinetics [7]
V_{max} (pmol/min/mg)	970	
K_m (µM)	3.3	
fu_{mic}	0.25	as above
rhUGT Scalar – Liver	5.26	
rhUGT Scalar – Intestine	0	
rhUGT Scalar – Kidney	0	
SULT		modelled as (microsomal) CES
CL_{int} (µL/min/mg)	224	optimized (initial guess: 5.4)
fu_{inc}	0.5	see text
Tissue Scalar – Liver	1	
Tissue Scalar – Intestine	0	
Tissue Scalar – Kidney	0	
CL_{renal} (L/h)	1.6	see text

Table 2
Physicochemical properties, blood and ADME parameters of BPAG and BPAS.

Parameter	Input value for BPAG	Input value for BPAS	Source / Comment
Physicochemical properties			
MW (g/mol)	404.415	308.4	Pubchem
log *P*	2.1	3.57	calculated in MarvinSketch
pK_a	3.25, 10 (diprotic acid)	0, 10 (diprotic acid)	calculated in MarvinSketch
Blood			
B/P ratio	1	1	default in Simcyp
fu_p	0.062	0.019	predicted according to [8], predominantly binding to HSA
Distribution			
Model	Minimal PBPK model	Minimal PBPK model	
V_{ss} (L/kg)	0.13	0.12	Rodgers and Rowland method (Simcyp Method 2)
Elimination			
CL_{renal} (L/h)	11	2	initial guess (BPAG), optimized (BPAS)

Table 3
Parameters for the first-order absorption model for oral administration.

Parameter	Input value	Source
f_a	1	[3]
k_a(1/h)	0.65	optimized (initial guess: 1.3)
Lag time (h)	0	default in Simcyp
fu_{gut}	1	recommended value for the Q_{gut} model
Q_{gut} (L/h)	18.4	calculated from $P_{eff,man}$
$P_{eff,man}$(10^{-4} cm/s)	10.1	predicted by the MechPeff model

Table 4
Trial design parameters of the selected clinical studies with oral administration.

Study	No. of subjects in trial	Proportion of females	Age (years)	Dose (mg/kg)	Dosage form
Thayer et al. [3]	14	0.57	26 – 46	0.1	cookie
Teeguarden et al. [4]	10	0	21 – 45	0.03	tomato soup

Table 5
Optimized ADME parameters for BPA and BPAG when using the advanced dissolution, absorption and metabolism (ADAM) model for oral administration.

Compound	Parameter	Input value	Source / Comment
BPA	*Absorption*		
	$P_{eff,man}$ (10^{-4} cm/s)	2.84	predicted from PSA and HBD
	Elimination via UGT1A9		
	rhUGT Scalar – Intestine	2.44	optimized (changed from 0.61)
BPAG	*Elimination (renal clearance)*		
	CL_{renal} (L/h)	8	see text
	Elimination (biliary clearance)		
	$CL_{int,bile}$ (µL/min/10^6 cells)	3	see text
	Elimination (Deconjugation in gut lumen)		
	$CL_{int,gutlumen}$ (µL/h/g of total luminal gut content)	10	see text

For PBPK model refinement and verification, we used the observed serum concentration-time profiles and cumulative urinary excretion-time profiles from the clinical studies of Thayer et al. [3] and Teeguarden et al. [4]. The model predictions with the first-order oral absorption model are shown in our companion paper [1]. The model predictions with the ADAM model are shown in Figs. 1 and 2. Results of a local sensitivity analysis for the PBPK model with first-order oral absorption model involving the blood-binding and ADME-related input parameters of Tables 1 and 2 are shown in Fig. 3.

The parameter dataset, the observed and predicted data, the Simcyp workspaces, and an R script used to generate the Figs. 1 and 2 are available from Mendeley Data repository.

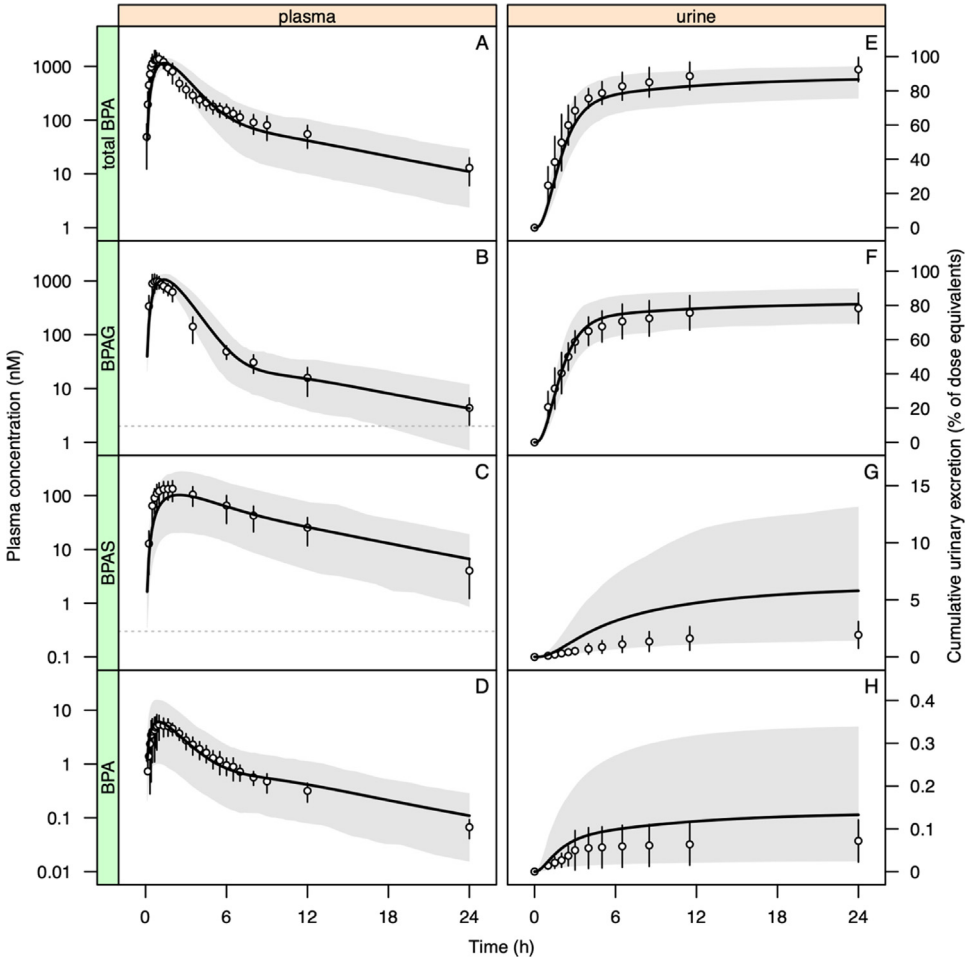

Fig. 1. Simulation of oral toxicokinetics of BPA by using the PBPK model with the advanced dissolution, absorption and metabolism (ADAM) model for the oral route. The thick solid lines show the population means of the predicted plasma concentration time profiles (left column) and the cumulative urinary excretion profiles (right column) of unconjugated, sulfated (BPAS), glucuronidated (BPAG), and total BPA. The gray-shaded areas indicate the predicted 5th to 95th percentile ranges. The observed data are shown as circles with error bars (mean ± standard deviation) and were taken from the toxicokinetic study of Thayer et al. [3], in which subjects ingested deuterated BPA in a cookie at a dose of 0.1 mg/kg BW. The limits of detection are indicated by dashed lines.

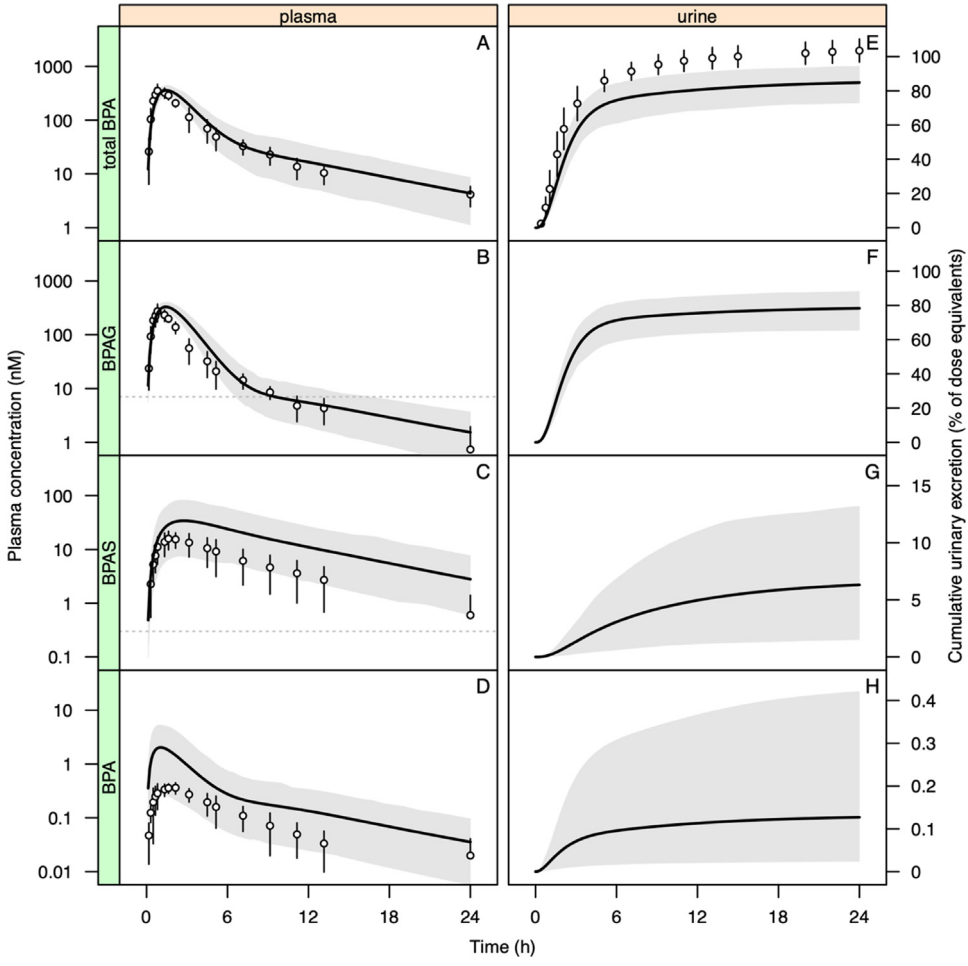

Fig. 2. Performance verification of the PBPK model with the ADAM model for the oral route. Circle symbols with error bars represent the mean ± standard deviation of the observed data from the toxicokinetic study of Teeguarden et al. [4], in which subjects ingested deuterated BPA in a soup at a dose of 0.03 mg/kg BW. For further details, see Fig. 1.

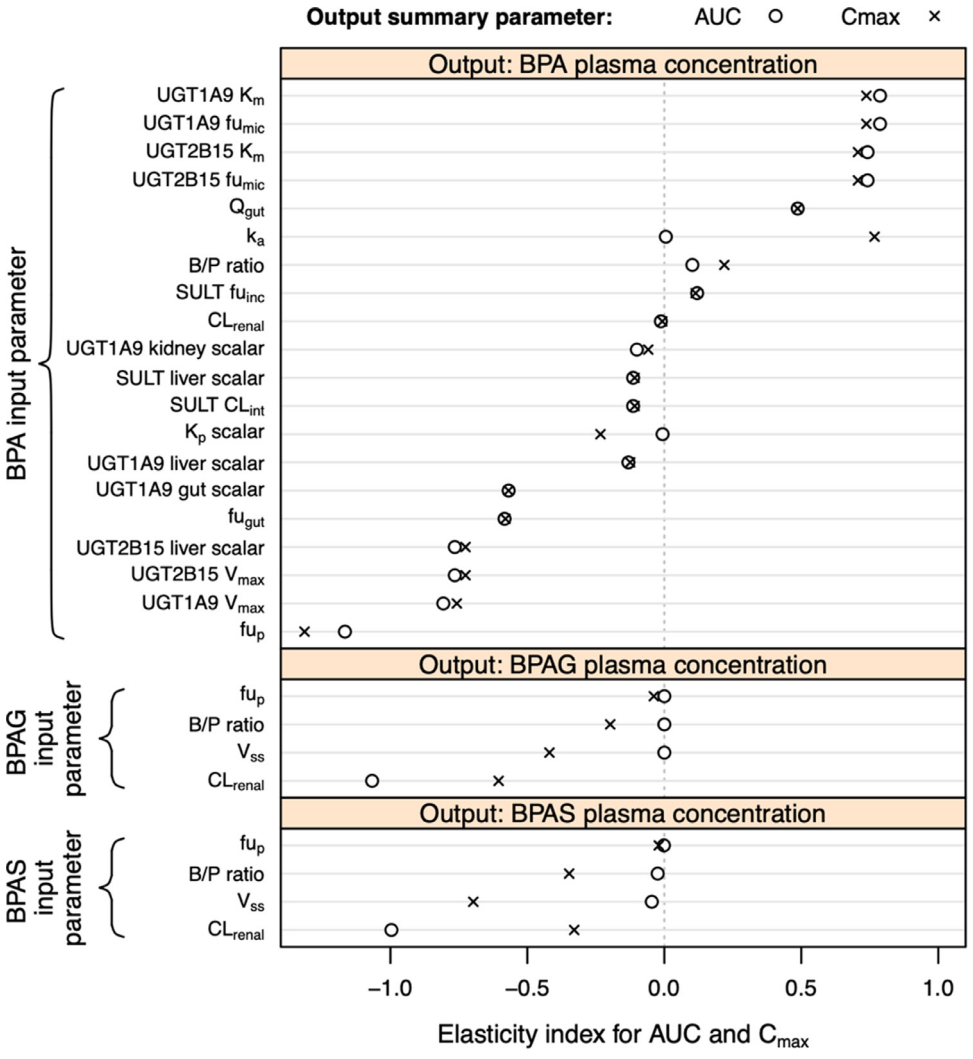

Fig. 3. Local sensitivity analysis for the PBPK model with the first-order model for the oral route. The figure visualizes how a small variation of an ADME-related or blood-binding input parameter (from Tables 1 and 2) around its initial value translates into changes in the outcome summary parameters AUC and C_{max} for the plasma concentrations of BPA, BPAG, and BPAS. This influence is quantified by the elasticity index.

3. Experimental Design, Materials and Methods

3.1. Physicochemical and ADME parameters

The physicochemical properties of BPA, BPAG, and BPAS, along with other compound-dependent parameters – the data required for compounds model development – were collected from the literature and databases, calculated in MarvinSketch 18.30.0 (http://www.chemaxon.com), or predicted by the use of Simcyp built-in QSAR models.

The PBPK model was set up in Simcyp® Simulator V21 (Certara UK, UK), which is a qualified platform for *in vitro* to *in vivo* extrapolation (IVIVE) and ADME data-based predictions of the toxicokinetics accounting for population variability. In the software, BPAG was configured as primary metabolite 1, and BPAS as primary metabolite 2.

BPA: The full-PBPK model structure was chosen as distribution model for BPA in Simcyp. The volume of distribution at steady-state (V_{ss}) was calculated from the tissue-to-plasma partition coefficients (K_p values) and the physiological tissue and plasma volumes. The K_p values were predicted by mechanistic equations of the Rodgers and Rowland method [9]. Comparison of the thus derived V_{ss} with a value predicted for humans from animal data [6] *via* allometric scaling revealed that the derived V_{ss} was too high. A K_p scalar of 0.42 was therefore applied to all K_p values to arrive at a V_{ss} of 1.8 L/kg (i.e., 125.3 L for a 70-kg human) for humans (Table 1).

Several reports on *in vitro* BPA elimination kinetics were identified. Most of the experiments were performed with human liver microsomes and hepatocytes. As a simulation of the metabolite kinetics requires enzyme-specific data, it was decided to use the kinetic data on the recombinant human UDP-glucuronosyltransferases UGT1A9 and UGT2B15 (Table 1), which were identified by Street et al. [7] as hepatic UGTs showing the highest BPA glucuronidation activity. Information on the fraction unbound in the *in vitro* microsomal incubation (fu_{mic}) was not available. Street et al. [7], however, used recombinant UGT (and microsomal) protein concentrations of 0.01–0.5 mg/mL, from which one can predict fu_{mic} values of 0.97–0.42 (Austin and Halifax equation 1) and of 0.99–0.72 (Austin and Halifax equation 2) [10] applicable to a compound with a log *P* (octanol:water partition coefficient) of 3.32. Corbel et al. [11] used sheep liver microsomes (1 mg/mL) and measured an fu_{mic} of 0.26, which one can translate according to Austin et al. [12] into fu_{mic} values of 0.42 and 0.97 for microsomal concentrations (mg/L) of 0.5 and 0.01, respectively. As an initial guess, an fu_{mic} of 0.5 was assumed.

The enzyme activity of each recombinant human UGT (rhUGT) was normalized to that of the native UGT in human liver tissue by using the relative activity factor (RAF) approach. The RAF is determined with a UGT-specific probe substrate (e.g., propofol for UGT1A9 and S-oxazepam for UGT2B15) by dividing the unbound intrinsic clearance in human liver microsomes by that in the rhUGT. For UGT1A9 and UGT2B15, Street et al. [7] determined RAF values of 3.22 and 5.26, respectively, which were used as rhUGT liver scalars (Table 1). The rhUGT tissue scalars for the kidney and intestine were obtained by multiplying the liver scalars by the kidney-to-liver and small intestine-to-liver UGT abundance ratios. For UGT1A9, abundance ratios of 8.21 (kidney-to-liver) and 0.61 (small intestine-to-liver) were calculated from the enzyme's absolute abundances of 31, 79, and 5.9 pmol/mg protein (extensive metabolizer [EM] phenotype) in the liver, kidney, and small intestine of the virtual "Sim-Healthy Volunteer" population. These absolute UGT1A9 abundances are consistent with literature values [13]. For UGT2B15, rhUGT scalars for kidney and intestine were set to zero since the absolute abundances in these tissues are close to zero.

Enzyme-specific data for the conjugation of BPA by sulfotransferases (SULTs) were not available. Kinetic data on BPA sulfation were therefore taken from Kurebayashi et al. [14], who studied the metabolic clearance of BPA in cryopreserved human hepatocytes. For the BPAS formation, they determined a maximum velocity (V_{max}) of 1.2 nmol/h/10^6 cells and a Michaelis-Menten constant (K_m) 10.1 µM, which translates into an *in vitro* intrinsic clearance ($CL_{int} = V_{max}/K_m$) of 2 µL/min/10^6 cells. For software-specific reasons, it was not possible to set up the sulfation under the "Cytosolic Enzymes" panel to enable the formation of BPAS as primary metabolite 2. As a workaround and surrogate of cytosolic enzyme, we selected the microsomal carboxylesterase

(CES) under the "Esterases" panel and adjusted the IVIVE parameters accordingly. By taking the Simcyp predictions of 107×10^6 hepatocytes per gram of liver (HPGL) and 39.5 mg microsomal protein per gram of liver (MPPGL) for a 33-year old subject (center of the age range in Thayer et al. [3]), the hepatocyte clearance translated into a microsomal *in vitro* intrinsic clearance (CL_{int}) of 5.4 µL/min/mg, which was used as an initial guess (Table 1). Since experimental information on the fraction unbound in the *in vitro* incubation (fu_{inc}) was not available, a value of 0.5 was predicted according to Austin et al. [15] for a compound with a log *P* of 3.32. The tissue scalar for the liver was kept at the default of 1, whereas those for the kidney and the small intestine were set to zero.

For the renal clearance (CL_{renal}) of (unconjugated) BPA, a value of 1.6 L/h was assumed as a typical value for a 20–30 year-old healthy male in Simcyp. This initial guess was obtained by dividing the total amount excreted by the area under the serum concentration-time curve (AUC) reported for the study population (26–45 years old, proportion of females: 0.6) in Thayer et al. [3].

A first check of the appropriateness of the elimination parameter values was done by comparing the predicted systemic plasma clearance following intravenous (IV) bolus injection with the IV clearance allometrically scaled from animals. Using the representative (male, 24 years old, body weight [BW] of 81 kg) of the virtual "Sim-Healthy Volunteer" population, the IV bolus injection of BPA at a dose of 0.1 mg/kg BW resulted in systemic plasma clearance of 89 L/h (with relative contributions of 90% from liver metabolism, 8% from kidney metabolism, and 2% from renal clearance). Allometric scaling approaches yield, however, higher serum clearances of 140 L/h ($= 5.264 \times BW^{0.749}$; [6]) and 123 L/h ($= 2.34 \times BW^{0.9014}$; [16]), respectively, for an 81-kg human. A parameter value refinement was, therefore, necessary at this stage of model development to approach these systemic plasma clearance estimates. This optimization was achieved by reducing the fu_{mic} for both UGTs to 0.25 (Table 1). The 50% reduction in fu_{mic} increased the systemic plasma clearance to an acceptably high value of 104 L/h (with relative contributions of 85.8% from liver metabolism, 12.6% from kidney metabolism, and 1.6% from renal clearance).

BPAG: The minimal PBPK model structure was chosen as a distribution model for BPAG. Fraction unbound in plasma (fu_p) and the volume of distribution at steady-state (V_{ss}) were predicted by the model of Lobell and Sivarajah [8] and by the Rodgers and Rowland method, respectively (Table 2). The rate of BPAG formation equalled the rate of BPA elimination *via* UGT-mediated pathway. BPAG is eliminated predominantly with urine in humans [3,4]. For the renal clearance (CL_{renal}), an initial guess of 11 L/h was calculated from the total amount excreted and the AUC reported in Thayer et al. [3].

BPAS: The minimal PBPK model structure was chosen as distribution model for BPAS. The parametrization was analogous to that for BPAG (Table 2). BPAS is a diprotic acid, for which MarvinSketch predicted pK_a values of –1.79 and 10, the lower one of which was entered as zero (lower bound in Simcyp). For the renal clearance (CL_{renal}), an initial guess of 1 L/h was calculated from the total amount excreted and the AUC reported in Thayer et al. [3].

3.2. Parameters for the oral route of administration

BPA absorption was simulated with the use of the first-order oral absorption model implemented in Simcyp. The toxicokinetic data of Thayer et al. [3] were used to estimate oral absorption parameters (Table 3). The fraction absorbed (f_a) was set to 1 (upper bound), since 84–109% of the oral dose of BPA was recovered in the urine of the study participants [3]. To account for the population variability in oral absorption, a coefficient of variation of 20% (default: 30%) was assumed for f_a. An initial estimate of 1.3 h^{-1} for the absorption rate constant (k_a) was derived from the absorption half-life of 0.52 h, which Thayer et al. [3] determined by noncompartmental pharmacokinetic analysis.

Intestinal first-pass metabolism was accounted for by the Q_{gut} model implemented in Simcyp. This model enables to predict the fraction of BPA escaping gut metabolism (F_g) from the net intrinsic metabolic clearance in the gut ($CLu_{int,G}$) based on unbound BPA concentration, the

fraction of BPA unbound in the enterocyte (fu_{gut}), and from Q_{gut}, which is a hybrid parameter of both permeability through the enterocyte membrane (CL_{perm}) and villous blood flow. The permeability clearance CL_{perm} is obtained by multiplying the effective intestinal permeability in human ($P_{eff,man}$) by the net cylindrical surface area of the small intestine.

Initial estimates for fu_{gut} were 0.004 (predicted by Simcyp built-in QSAR model) and 1, the latter being the recommended value. Different approaches are available to estimate $P_{eff,man}$. It can be predicted from molecular descriptors – the polar surface area (PSA) and the number of hydrogen bond donors (HBD) – using a QSAR model established with human *in vivo* data [17]. For BPA, a PSA of 40.42 $Å^2$ (square ångströms) and an HBD of 2 was calculated by using MarvinSketch 18.30.0, which translates into a $P_{eff,man}$ of 2.84 $\times$ 10^{-4} cm/h. $P_{eff,man}$ can also be predicted from the apparent permeability (P_{app}) of BPA in Caco-2 cell monolayers. Kamiya et al. [18] measured a P_{app} of 32.1 $\times$ 10^{-6} cm/s (apical and basolateral pH 7.4) which translates into a $P_{eff,man}$ of 3.8 $\times$ 10^{-4} cm/h. Punt et al. [19] measured a P_{app} of 72 $\times$ 10^{-6} cm/s (apical pH 6.5 and basolateral pH 7.4) which gave a $P_{eff,man}$ of 8.4 $\times$ 10^{-4} cm/h. The Mechanistic Permeability ('MechPeff') model [20] predicts a $P_{eff,man}$ of 10.1 $\times$ 10^{-4} cm/h. This value was used as initial estimate, which translates into a Q_{gut} value of 18.4 L/h (Table 3).

For PBPK model predictions, 10 virtual trials were simulated using the sample size, proportion of females, age range, and dose of the respective clinical study populations (Table 4). North European healthy volunteers' specific physiological parameters were used for all simulations.

Running the PBPK model with the initial parameter estimates for the first-order absorption model, and using the trial design of the oral toxicokinetic study of Thayer et al. [3] (Table 4), resulted in a quite good prediction of the plasma concentration-time profiles for BPAG and total BPA. The plasma level for BPA was, however, overpredicted, and that for BPAS underpredicted. Increasing fu_{gut} from 0.004 to the recommended value of 1 resulted in a higher intestinal extraction (F_g decreased from 0.99 to 0.46). The BPA plasma concentration was predicted well for times greater than 3 h post-dosing, but overpredicted for earlier time points. The absorption rate constant (k_a) was therefore manually fitted to approximate the observed C_{max} of Thayer et al. [3]. The procedure resulted in a k_a value of 0.65 h^{-1} (Table 3). The final refinement in model parameters comprised the 40-fold increase in the hepatic sulfation clearance (Table 1) and the doubling of the renal clearance of BPAS from 1 to 2 L/h (Table 2) to improve the prediction of BPAS plasma levels. Reducing $P_{eff,man}$ from 10.1 to 2.84 $\times$ 10^{-4} cm/h had only a marginal impact on BPA plasma levels, so it was decided to keep the initial $P_{eff,man}$ value. The predictions for the first-order absorption model with the final (i.e., refined) parameter estimates are shown in in our companion paper [1].

Overall, there was a good agreement between the observed data and the predicted plasma levels of BPA, BPAS, BPAG, and total BPA. However, the model predictions showed some deviations from the observed plasma concentration-time profiles in the first hours post-dosing for BPA and BPAG as well as in the terminal phase for BPAG [1]. To improve the predictions, we replaced the first-order oral absorption model by the advanced dissolution, absorption and metabolism (ADAM) model in Simcyp. This replacement made it necessary to optimize two ADME parameter for BPA: $P_{eff,man}$ was reduced from 10.1 to 2.84 $\times$ 10^{-4} cm/h, and the rhUGT scalar for UGT1A9 in the intestine was changed from 0.61 to 2.44 to increase the glucuronidation of BPA in the enterocytes (Table 5). To capture the slowed systemic clearance of BPAG and BPA in the terminal phase, we activated enterohepatic recirculation (EHR) by attributing a certain portion of the systemic renal clearance of BPAG to biliary clearance and by enabling the back-conversion of BPAG into BPA in the gut lumen. The CL_{renal} for BPAG was reduced from 11 to 8 L/h, and the *in vitro* intrinsic biliary clearance ($CL_{int,bile}$) was set to 3 µL/min/10^6 cells (Table 5). The intestinal luminal intrinsic clearance of ($CL_{int,gutlumen}$) was set to 10 µL/h per g of total luminal gut content (Table 5). This value was chosen to be high enough to ensure that the biliary excreted BPAG is sufficiently cleaved into BPA during the intestinal passage so that released BPA can be reabsorbed from the gut lumen.

For the average subject of the simulated study population of Thayer et al. [3] (33 years old, 72.5 kg body weight), the *in vitro* intrinsic biliary clearance ($CL_{int,bile}$) for BPAG translates into an (unbound) intrinsic biliary clearance of 30 L/h when assuming for HPGL a value of 107 $\times$ 10^6

cells/g liver and a liver weight of 1575 g. Based on the well-stirred liver model, and by assuming a liver blood flow of 84 L/h and using the fraction unbound in plasma and the blood-to-plasma ratio for BPAG (Table 2), unbound intrinsic biliary clearance translates into a systemic biliary clearance of 1.8 L/h.

The PBPK model predictions with the ADAM model for the oral route for the data of Thayer et al. [3] are shown in Fig. 1. PBPK model performance verification was carried out by simulating the toxicokinetic study of Teeguarden et al. [4], for which the trial design information is given in Table 4. The results of the model performance verification are shown in Fig. 2.

In order to identify the input parameters that are the most influential on the simulation results, a local sensitivity analysis was performed for the PBPK model with the first-order absorption model for the oral route. The ADME-related and blood-binding parameters of Tables 1 and 2 were used as input parameters, and the AUC and C_{max} for the plasma concentrations of BPA, BPAG, and BPAS were used as output summary parameters. The elasticity index was used as a normalized sensitivity measure [1]. Fig. 3 visualizes how a small variation of an input parameter around its initial (i.e., nominal) value translates into changes in the outcome summary parameters.

Ethics Statements

Not applicable.

CRediT Author Statement

Barbara Wiśniowska: Conceptualization, Methodology, Data curation, Investigation, Writing – original draft, Writing – review & editing; **Susanne Linke:** Project administration, Data curation, Writing – review & editing; **Sebastian Polak:** Conceptualization, Writing – review & editing, Supervision; **Zofia Bielecka:** Data curation, Writing – review & editing; **Andreas Luch:** Writing – review & editing; **Ralph Pirow:** Conceptualization, Methodology, Writing – original draft, Writing – review & editing, Visualization, Supervision, Project administration.

Declaration of Competing Interest

Sebastian Polak and Zofia Bielecka are Certara UK (Simcyp Division) employees. All other authors declare that they have no known competing financial interests or personal relationships that could have appeared to influence the work reported in this paper.

Data Availability

Data for: Data on ADME parameters of bisphenol A and its metabolites for use in physiologically based pharmacokinetic modelling (Original data) (Mendeley Data).

Acknowledgments

The present study was financially supported by the German Federal Institute for Risk Assessment (BfR) (grant number 1329-572). The authors would like to thank Justin Teeguarden for providing the raw data of toxicokinetic study in humans involving the oral administration of BPA.

References

[1] B. Wisniowska, S. Linke, S. Polak, Z. Bielecka, A. Luch, R. Pirow, Physiologically based modelling of dermal absorption and kinetics of consumer-relevant chemicals: A case study with exposure to bisphenol A from thermal paper, Toxicol. Appl. Pharmacol. 459 (2023) 116357, doi:10.1016/j.taap.2022.116357.

[2] M. Jamei, D. Turner, J. Yang, S. Neuhoff, S. Polak, A. Rostami-Hodjegan, G. Tucker, Population-based mechanistic prediction of oral drug absorption, AAPS J. 11 (2) (2009) 225–237, doi:10.1208/s12248-009-9099-y.

[3] K.A. Thayer, D.R. Doerge, D. Hunt, S.H. Schurman, N.C. Twaddle, M.I. Churchwell, S. Garantziotis, G.E. Kissling, M.R. Easterling, J.R. Bucher, L.S. Birnbaum, Pharmacokinetics of bisphenol A in humans following a single oral administration, Environ. Int. 83 (2015) 107–115, doi:10.1016/j.envint.2015.06.008.

[4] J.G. Teeguarden, N.C. Twaddle, M.I. Churchwell, X. Yang, J.W. Fisher, L.M. Seryak, D.R. Doerge, 24-hour human urine and serum profiles of bisphenol A: Evidence against sublingual absorption following ingestion in soup, Toxicol. Appl. Pharmacol. 288 (2) (2015) 131–142, doi:10.1016/j.taap.2015.01.009.

[5] G.A. Csanady, H.R. Oberste-Frielinghaus, B. Semder, C. Baur, K.T. Schneider, J.G. Filser, Distribution and unspecific protein binding of the xenoestrogens bisphenol A and daidzein, Arch. Toxicol. 76 (5-6) (2002) 299–305, doi:10.1007/s00204-002-0339-5.

[6] C.Y. Cho, B.S. Shin, J.H. Jung, D.H. Kim, K.C. Lee, S.Y. Han, H.S. Kim, B.M. Lee, S.D. Yoo, Pharmacokinetic scaling of bisphenol A by species-invariant time methods, Xenobiotica 32 (10) (2002) 925–934, doi:10.1080/00498250210163315.

[7] C.M. Street, Z. Zhu, M. Finel, M.H. Court, Bisphenol-A glucuronidation in human liver and breast: identification of UDP-glucuronosyltransferases (UGTs) and influence of genetic polymorphisms, Xenobiotica 47 (1) (2017) 1–10, doi:10.3109/00498254.2016.1156784.

[8] M. Lobell, V. Sivarajah, In silico prediction of aqueous solubility, human plasma protein binding and volume of distribution of compounds from calculated pKa and AlogP98 values, Mol. Divers. 7 (1) (2003) 69–87, doi:10.1023/b:modi.0000006562.93049.36.

[9] T. Rodgers, M. Rowland, Physiologically based pharmacokinetic modelling 2: Predicting the tissue distribution of acids, very weak bases, neutrals and zwitterions, J. Pharmaceut. Sci. 95 (6) (2006) 1238–1257, doi:10.1002/jps.20502.

[10] M. Gertz, P.J. Kilford, J.B. Houston, A. Galetin, Drug lipophilicity and microsomal protein concentration as determinants in the prediction of the fraction unbound in microsomal incubations, Drug. Metab. Dispos. 36 (3) (2008) 535–542, doi:10.1124/dmd.107.018713.

[11] T. Corbel, E. Perdu, V. Gayrard, S. Puel, M.Z. Lacroix, C. Viguie, P.L. Toutain, D. Zalko, N. Picard-Hagen, Conjugation and deconjugation reactions within the fetoplacental compartment in a sheep model: a key factor determining bisphenol A fetal exposure, Drug. Metab. Dispos. 43 (4) (2015) 467–476, doi:10.1124/dmd.114.061291.

[12] R.P. Austin, P. Barton, S.L. Cockroft, M.C. Wenlock, R.J. Riley, The influence of nonspecific microsomal binding on apparent intrinsic clearance, and its prediction from physicochemical properties, Drug. Metab. Dispos. 30 (12) (2002) 1497–1503, doi:10.1124/dmd.30.12.1497.

[13] J.M. Hutzler, M.A. Zientek, Non-cytochrome P450 enzymes and glucuronidation, in: A.G.E. Wilson (Ed.), New horizons in predictive drug metabolism and pharmacokinetics, The Royal Society of Chemistry, Cambridge, 2016, pp. 79–130.

[14] H. Kurebayashi, K. Okudaira, Y. Ohno, Species difference of metabolic clearance of bisphenol A using cryopreserved hepatocytes from rats, monkeys and humans, Toxicol. Lett. 198 (2) (2010) 210–215, doi:10.1016/j.toxlet.2010.06.017.

[15] R.P. Austin, P. Barton, S. Mohmed, R.J. Riley, The binding of drugs to hepatocytes and its relationship to physicochemical properties, Drug. Metab. Dispos. 33 (3) (2005) 419–425, doi:10.1124/dmd.104.002436.

[16] S.H. Collet, N. Picard-Hagen, M.Z. Lacroix, S. Puel, C. Viguie, A. Bousquet-Melou, P.L. Toutain, V. Gayrard, Allometric scaling for predicting human clearance of bisphenol A, Toxicol. Appl. Pharmacol. 284 (3) (2015) 323–329, doi:10.1016/j.taap.2015.02.024.

[17] S. Winiwarter, N.M. Bonham, F. Ax, A. Hallberg, H. Lennernas, A. Karlen, Correlation of human jejunal permeability (in vivo) of drugs with experimentally and theoretically derived parameters. A multivariate data analysis approach, J. Med. Chem. 41 (25) (1998) 4939–4949, doi:10.1021/jm9810102.

[18] Y. Kamiya, H. Takaku, R. Yamada, C. Akase, Y. Abe, Y. Sekiguchi, N. Murayama, M. Shimizu, M. Kitajima, F. Shono, K. Funatsu, H. Yamazaki, Determination and prediction of permeability across intestinal epithelial cell monolayer of a diverse range of industrial chemicals/drugs for estimation of oral absorption as a putative marker of hepatotoxicity, Toxicol. Rep. 7 (2020) 149–154, doi:10.1016/j.toxrep.2020.01.004.

[19] A. Punt, A. Aartse, T.F.H. Bovee, A. Gerssen, S.P.J. van Leeuwen, R. Hoogenboom, A. Peijnenburg, Quantitative in vitro-to-in vivo extrapolation (QIVIVE) of estrogenic and anti-androgenic potencies of BPA and BADGE analogues, Arch. Toxicol. 93 (7) (2019) 1941–1953, doi:10.1007/s00204-019-02479-6.

[20] D. Pade, M. Jamei, A. Rostami-Hodjegan, D.B. Turner, Application of the MechPeff model to predict passive effective intestinal permeability in the different regions of the rodent small intestine and colon, Biopharm. Drug. Dispos. 38 (2) (2017) 94–114, doi:10.1002/bdd.2072.